

Single Crystal Diamond Refractive Lens for Focusing of X-rays in Two Dimensions

S. Antipov^{1*}, S.V. Baryshev¹, J.E. Butler^{1,4}, O. Antipova², Z. Liu³, S. Stoupin^{3**}

¹ Euclid Techlabs LLC, Solon, OH 44139 USA

² Department of Biological and Chemical Sciences, Illinois Institute of Technology, Chicago, IL 60616 USA

³ Advanced Photon Source, Argonne National Laboratory, Lemont, IL 60439 USA

⁴ Institute of Applied Physics of the Russian Academy of Sciences, Nizhny Novgorod, Russia

Abstract:

We report the fabrication and performance evaluation of single crystal diamond refractive x-ray lenses with a paraboloid of rotation form factor for focusing x-rays in two dimensions simultaneously. The lenses were manufactured using a femtosecond laser micromachining process and tested using x-ray synchrotron radiation. Such lenses can be stacked together to form a traditional compound refractive lens (CRL). Due to the superior physical properties of the material, diamond CRLs are enabling and indispensable wavefront-preserving primary focusing optics for x-ray free-electron lasers and the next-generation synchrotron storage rings. They can be used for highly efficient refocusing of the extremely bright x-ray sources on secondary optical schemes with limited aperture such as nanofocusing Fresnel zone plates and multilayer Laue lenses.

* s.antipov@euclidtechlabs.com

** sstoupin@aps.anl.gov

The next generation light sources such as diffraction-limited storage rings and high repetition rate free electron lasers will generate x-ray beams with significantly increased peak and average brilliance. These future facilities will require x-ray optical components capable of handling large instantaneous and average power density while tailoring the properties of the x-ray beams for a variety of scientific experiments.

Since the invention of x-ray compound refractive lenses (CRL) in the 90s [1] refractive x-ray optics has become one of the basic optical elements which couples the primary radiation of the highly brilliant x-ray sources with a variety of x-ray instruments to probe matter on the atomic level. Among the advantages of refractive x-ray optics are the preservation of the x-ray beam trajectory, robustness, compactness and relaxed requirements on surface quality owing to the transmission geometry. Commercially available polycrystalline beryllium refractive lenses with parabolic profiles [2, 3] are successfully used at the third-generation synchrotrons to refocus the

x-ray source onto downstream optics, and, also as transfocators (reconfigurable stacks of CRLs) for selection of a photon bandwidth which is comparable to the bandwidth of high-brilliance undulator-based x-ray source [4, 5].

However, the choice of polycrystalline beryllium (dictated by very limited availability of high-quality single crystal material) results in limitations. These are the presence of grain boundaries which may distort the radiation wavefront, radiation damage limitations and environmental concerns (beryllium is highly toxic). The performance of a refractive lens can be improved by minimization of scattering from intrinsic inhomogeneities via a choice of material with low small angle scattering [2]. This also suggests preference of a single crystal over a polycrystalline material for lens fabrication. It is therefore imperative to develop the next-generation x-ray optics suitable for operation at the increased levels of x-ray power density.

Diamond has been the material of choice for several important high-heat-load applications in x-ray optics including double-crystal monochromators [6-8] and Bragg mirrors for the x-ray free-electron laser oscillator [9, 10]. Beyond that, it has been recently shown that diamond x-ray optics can withstand the direct x-ray free electron laser (XFEL) beam and provide the best performance parameters as Fresnel zone plates for nanofocusing of XFEL pulses [11], diffracting crystals for XFEL self-seeding [12, 13] and XFEL beam multiplexing [14, 15]. Theoretical studies (e.g., [16]) demonstrate that the present and future targets for instantaneous power densities are still below the radiation damage threshold in diamond. High average power density diamond resilience tests are currently in progress at the Advanced Photon Source [17].

Thus, the studies conducted so far demonstrate that diamond is an indispensable material for critical applications in x-ray optics for the present and the future light source facilities. A unique combination of exceptional intrinsic material properties such as high radiation hardness, record high thermal conductivity, small thermal expansion coefficient and uniformity of refractive index make single crystal diamond a material-of-choice for wavefront-preserving refracting optics in the critical *high-peak* and *high-average* power density applications. Several groups have reported successful fabrication and testing of diamond refractive lenses for focusing x-rays in one dimension (1D) [18-20]. These structures produced by ion/plasma etching have limited lateral apertures ≤ 100 μm , which is insufficient to accommodate the typical size of the high-brightness x-ray beams. Single crystal 1D diamond CRLs fabricated by laser micromachining to allow a suitable lateral aperture (~ 500 μm) have been recently demonstrated [21].

In this work, we report the results of fabrication and characterization of single crystal diamond refractive lenses based on the established and widely accepted paraboloid of rotation form factor [2, 3]. It was shown that such lenses are free of aberrations and focus x-rays in two directions [3]. Femtosecond laser micromachining was used to produce the paraboloids of a small local radius of curvature (~ 100 μm) in single crystal CVD diamond plates available commercially. The fabricated lenses were tested using synchrotron radiation by reimaging a photon source of a bending magnet beamline ($\sim 198 \times 78$ μm^2) to a plane located at a distance of 54 m from the source. Nearly theoretical transmission over the aperture 230 μm in diameter was demonstrated at the photon energy of 13.6 keV.

While the choice of diamond based on its physical properties is obvious, the practical implementation is challenging. Conventional laser cutting by a standard nanosecond diamond cutter lasers provides non-satisfactory results caused by thermal fatigue in diamond [22]. Unlike the conventional approach, femtosecond laser pulse duration is extremely short: the material is ablated and pulsed heating effects are minimized. The lenses presented here were manufactured from a single crystal CVD optical grade 587-microns-thick diamond plate. To machine a 2D paraboloid, the fs-laser beam was steered by a galvo mirror to ablate circle patterns gradually reducing the circle diameter with depth. The largest diameter on the diamond surface was of about 450 μm . Identically, a matching paraboloid was micromachined on the opposite side of the diamond plate (Figure 1). After micromachining diamonds were cleaned in a hot mineral acid bath.

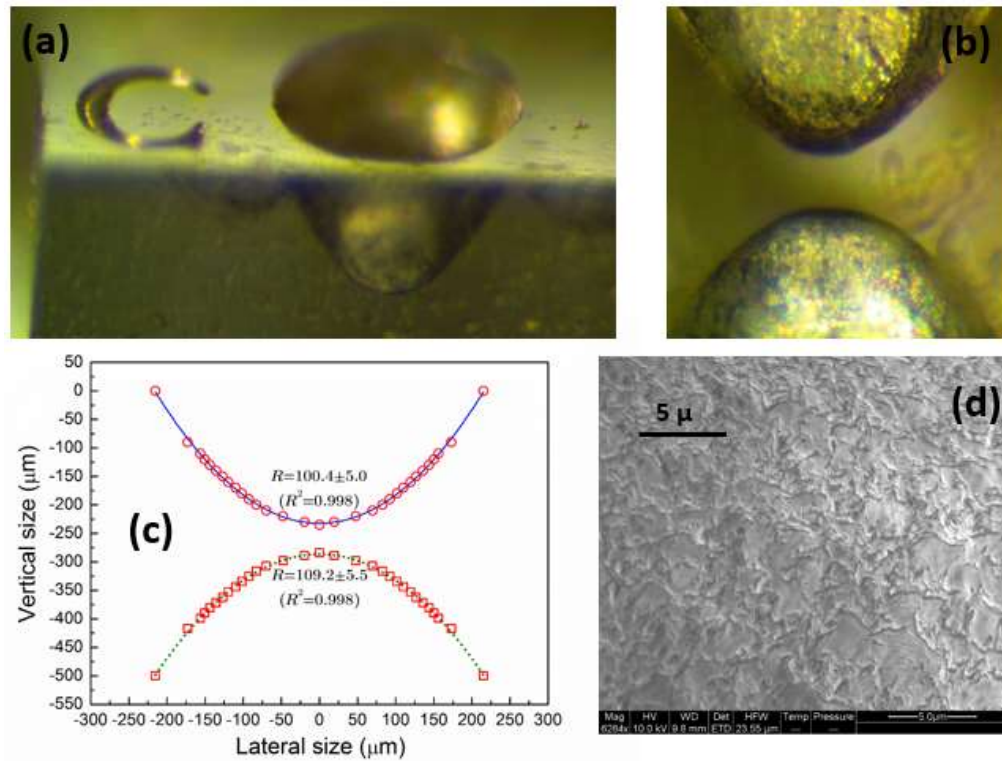


Figure 1. Microscope image of the lens at various angles (a, b). (c) Profile of the lens measured by an optical profilometer and parabolic fit with radii of curvature. (d) Scanning electron micrograph of the lens surface shows roughness on the order of 1 μm .

It was experimentally established, that about 40 μm distance (waist) can be left between the paraboloids. The diamond would get punctured when a thinner smaller paraboloid separation was attempted. Figure 1 (a, b) shows the lens profile image taken by an optical microscope. The parabolic shape can be seen through the transparent side of the diamond plate (Fig. 1a). Two paraboloids are depicted on Figure 1 (b), image taken from the side of the diamond plate. When the first paraboloid was machined on the diamond surface, the total depth of the cut was measured. The second paraboloid was machined with the laser power scaled to maintain the separation of at least 40 μm . This is why the paraboloids had different radii of curvature (100 and 109 μm) as measured by white light interferometry (WLI) using an optical profilometer MicroXAM-1200

[23]. WLI could not automatically reconstruct 3D profile of the lenses due to poor reflectivity in the direction normal to the surface and high diamond transparency. By combining objectives of different magnification and enhanced contrast imaging, interference fringe diameters at different vertical positions of the focal plane, with the diamond surface set to zero as a reference, were recorded. All fringes (representing 2D cross-sections of a 3D solid at every focal plane parallel to the surface) were quasi-circular confirming that the micro-machined lenses were paraboloids. Finally, curvature radii were measured via plotting a dependence of the fringe diameter on depth (symbols in Fig.1c) and fitting this dependence with a quadratic function (lines in Fig.1c). Goodness of determination (R^2) was 0.998.

The measured waist between the paraboloids in the tested lenses was 50 μm . Scanning electron microscopy image of the lens surface (Fig.1d) shows roughness on the order of 1 μm .

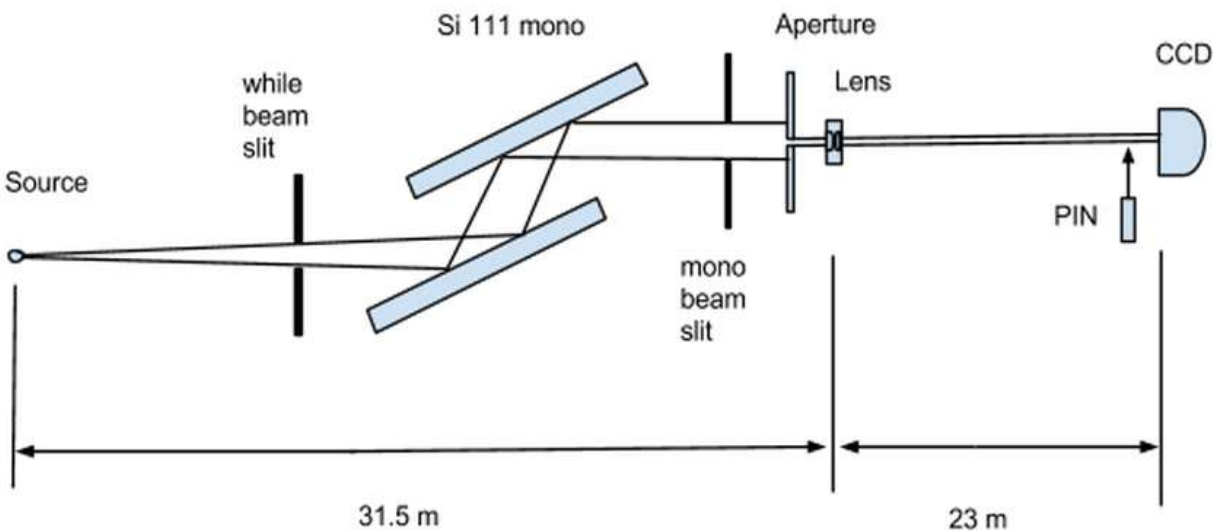


Figure 2. Experimental setup (see text for details).

The experiment was performed at 1-BM Optics testing beamline of the Advanced Photon Source. The experimental arrangement is shown in Fig.2. A Si 111 double crystal monochromator was tuned to photon energy of 14.4 keV. To limit the wavefront distortion caused by the heat load on the monochromator first crystal, the size of the incident white beam was set to $1 \times 1 \text{ mm}^2$ using the upstream white beam slit. The size of the monochromator exit beam was selected to be comparable with the total lens aperture using mono beam slits. The lenses were placed at a distance of 31.5 m from the source (bending magnet). A circular pinhole aperture with diameter $\sim 230 \mu\text{m}$ was placed in front of the lens. Imaging of the transmitted/refracted beam profile was performed using an area detector (CCD) placed at $\sim 23 \text{ m}$ downstream of the lens. A retractable solid state pin diode detector (PIN) was used for relative measurements of the lens transmission (lens in/out of the beam). The area detector was equipped with 250- μm -thick LUAG:CE scintillator and an objective lens with 10X magnification. The field of view for the area detector was $1.6 \times 1.4 \text{ mm}^2$ with the effective pixel size of $\sim 0.65 \mu\text{m}$.

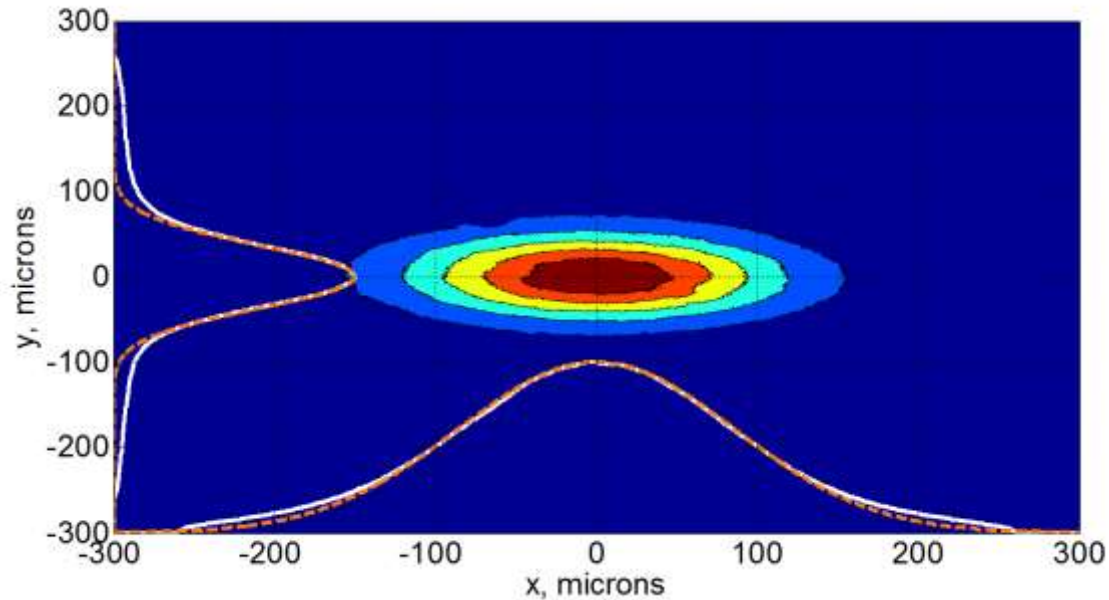


Figure 3. Image of the focused x-ray beam produced by a single lens at 13.6 keV. Beam projections on x and y axes (white, solid), gaussian fit (orange, dashed). The refocused source size is 183 micron \times 86 micron (FWHM).

In the experiment the bending magnet source size was reimaged to the far experimental station at the beamline while the lens was placed in the near station. The nominal demagnification ratio was 0.73. The bending magnet source size was $198(4) \times 78(1) \mu\text{m}^2$ full width at half maximum (FWHM). These values were taken equal to the corresponding electron beam sizes of the bending magnet source which were extracted from the log of synchrotron parameters.

Two different diamond samples were investigated; each had a 3×3 array of lenses. The two samples were of different single crystal CVD diamond grades. No substantial difference in the lens performance parameters was found for any of the lenses in the two samples. To arrive to the optimal refocusing geometry the photon energy of the monochromator was tuned to obtain a minimal size of the source in the imaging plane located at the fixed distance corresponding to the focal distance $f = 13.3$ m. The optimal photon energy was found to be 13.6 keV. The equation for the focal distance of the lens $f = R/(2 \cdot \delta(E))$ allows us to evaluate the effective radius of curvature R since the refractive decrement $\delta(E)$ is a tabulated value. The effective radius of curvature was found to be $R = 105 \mu\text{m}$, which is in good agreement with the results by optical profilometry (Fig. 1c).

In this optimal condition we measured the source image size by fitting a 2D Gaussian distribution to the intensity distribution in the imaging plane and transmission of the lens using the integrating detector. Because of the surface roughness and non-ideal paraboloid shape of the lens the reimaged source distribution slightly deviates from a gaussian shape (Fig. 3.). In order to compare experimental results with the theory the measured transmission value $T = 0.973$ was renormalized by the fraction of the signal forming the gaussian portion of the image. The obtained effective transmission T_{eff} was 0.87. The transverse distribution of the beam obtained with the area

detector and the gaussian fit projections are shown in Fig. 3. The measured and theoretical performance parameters are summarized in Table 1.

A relevant theoretical model describing transmission through the lens of material with refractive index $n = 1 - \delta - i \cdot \lambda\mu/(4\pi)$, where λ is the radiation wavelength, takes into account the interface roughness, σ . The effective transmission is given by [3]:

$$T = \frac{\exp(-\mu d)}{2a_p} [1 - \exp(-2a_p)] \quad (1)$$

The attenuation factor a_p is given by:

$$a_p = \frac{R_0^2}{2R^2} [\mu R + 2Q_0^2\sigma^2], \quad (2)$$

where $Q_0 = 2\pi d/\lambda$, is the momentum transfer for transmission through an air-lens interface at normal incidence. The distance between the lenses paraboloids is d .

This equation allows us to evaluate the transmission of the lens taking into account the surface roughness $\sigma = 1.0 \mu m$ estimated from the SEM measurements. The obtained value is $T = 0.89$ which agrees with the effective measured transmission $T_{eff} = 0.87$.

The gain of a refractive lens is defined as the ratio of the intensity in the focal spot to the intensity behind a pinhole ($2R_0 = 230 \mu m$) equal to the spot of the lens: $g = T_{eff} \cdot 4 \cdot R_0^2 / (B_v \cdot B_h)$ [3]. An ideal lens in the geometry shown in Fig.2 should refocus the source to an image with sizes $B_h = 145 \mu m$ and $B_v = 57 \mu m$, both FWHM. The obtained values are larger ($183 \mu m \times 86 \mu m$) which can be attributed to deviations of the lens profile from the ideal shape.

Table 1. Lens performance parameters.

E [keV]	T, theory	Gain, theory	T_{eff} , experiment	B_h , measured	B_v , measured	Gain, exp
13.6	0.89	5.71	0.87	183 μm	86 μm	2.83

We observe a difference in the measured and the theoretical gain similar to what was reported earlier in a one dimensional diamond lens [21]. The laser micromachining process featuring a step by step ablation of material produces a modulated parabolic profile that results in broadened focal spot and reduced gain [21].

In summary, a two-dimensional x-ray refractive lens was fabricated out of single crystal diamond and experimentally tested. Efficient refocusing of a bending magnet source to a nearly Gaussian beam profile was demonstrated at photon energy of 13.6 keV. Such lenses can be stacked together to form a traditional CRL. Femtosecond laser micromachining of diamond lenses is a promising approach that can be further refined to provide more accurate shapes and better surface finish. Diamond CRLs will become the main choice for x-ray focusing of primary beams at future light sources. Due to outstanding thermal and radiation hardness properties of diamond these

devices can withstand extremely high instantaneous flux densities generated by XFELs as well as unprecedented average flux densities of the next-generation light sources with high repetition rates.

We are indebted to K.-J. Kim, Yu.V. Shvyd'ko, C. Jacobsen and A. Sandy for helpful discussions on the topic of x-ray refractive optics. R. Woods and K. Lang are acknowledged for technical support. Euclid Techlabs LLC acknowledges support from DOE SBIR program grant No. DE-SC0013129. Use of the Advanced Photon Source was supported by the U. S. Department of Energy, Office of Science, Office of Basic Energy Sciences, under Contract No. DE-AC02-06CH11357. J.B. acknowledges the support of the Act 220 of the Russian Government (Agreement no. 14.B25.31.0021 with the host organization IAP RAS).

References:

- [1] A. Snigirev *et al.*, *A Compound Refractive Lens for Focusing High-Energy X-Rays*, *Nature* **384**, 49 (1996).
- [2] B. Lengeler *et al.*, *Transmission and Gain of Singly and Doubly Focusing Refractive X-Ray Lenses*, *Journal of Applied Physics* **84**, 5855 (1998).
- [3] B. Lengeler *et al.*, *Imaging by Parabolic Refractive Lenses in the Hard X-Ray Range*, *Journal of Synchrotron Radiation* **6**, 1153 (1999).
- [4] G. B. M. Vaughan *et al.*, *X-Ray Transfocators: Focusing Devices Based on Compound Refractive Lenses*, *Journal of Synchrotron Radiation* **18**, 125 (2011).
- [5] A. V. Zozulya *et al.*, *Microfocusing Transfocator for 1d and 2d Compound Refractive Lenses*, *Optics Express* **20**, 18967 (2012).
- [6] L. E. Berman *et al.*, *Diamond Crystal X-Ray Optics for High-Power-Density Synchrotron Radiation Beams*, *Nuclear Instruments and Methods in Physics Research Section A: Accelerators, Spectrometers, Detectors and Associated Equipment* **329**, 555 (1993).
- [7] A. K. Freund, *Diamond Single Crystals: The Ultimate Monochromator Material for High-Power X-Ray Beams*, *Optical Engineering* **34**, 432 (1995).
- [8] P. B. Fernandez *et al.*, *Test of a High-Heat-Load Double-Crystal Diamond Monochromator at the Advanced Photon Source*, *Nuclear Instruments and Methods in Physics Research Section A: Accelerators, Spectrometers, Detectors and Associated Equipment* **400**, 476 (1997).
- [9] Y. V. Shvyd'ko *et al.*, *High-Reflectivity High-Resolution X-Ray Crystal Optics with Diamonds*, *Nature Physics* **6**, 196 (2010).
- [10] Y. Shvyd'ko *et al.*, *Near-100% Bragg Reflectivity of X-Rays*, *Nature Photonics* **5**, 539 (2011).
- [11] C. David *et al.*, *Nanofocusing of Hard X-Ray Free Electron Laser Pulses Using Diamond Based Fresnel Zone Plates*, *Scientific Reports* **1** (2011).
- [12] J. Amann *et al.*, *Demonstration of Self-Seeding in a Hard-X-Ray Free-Electron Laser*, *Nature Photonics* **6**, 693 (2012).
- [13] S. Stoupin *et al.*, *Diamond Crystal Optics for Self-Seeding of Hard X-Rays in X-Ray Free-Electron Lasers*, *Diamond and Related Materials* **33**, 1 (2013).
- [14] S. Stoupin *et al.*, *All-Diamond Optical Assemblies for a Beam-Multiplexing X-Ray Monochromator at the Linac Coherent Light Source*, *Journal of Applied Crystallography* **47**, 1329 (2014).
- [15] D. Zhu *et al.*, *Performance of a Beam-Multiplexing Diamond Crystal Monochromator at the Linac Coherent Light Source*, *Review of Scientific Instruments* **85**, 063106 (2014).
- [16] N. Medvedev *et al.*, *Nonthermal Graphitization of Diamond Induced by a Femtosecond X-Ray Laser Pulse*, *Physical Review B* **88** (2013).
- [17] K. Kim and Y. V. Shvyd'ko, private communication.
- [18] B. Nöhammer *et al.*, *Diamond Planar Refractive Lenses for Third- and Fourth-Generation X-Ray Sources*, *Journal of Synchrotron Radiation* **10**, 168 (2003).
- [19] A. F. Isakovic *et al.*, *Diamond Kinoform Hard X-Ray Refractive Lenses: Design, Nanofabrication and Testing*, *Journal of Synchrotron Radiation* **16**, 8 (2008).
- [20] L. Alianelli *et al.*, *A Planar Refractive X-Ray Lens Made of Nanocrystalline Diamond*, *Journal of Applied Physics* **108**, 123107 (2010).
- [21] M. Polikarpov *et al.*, *X-Ray Harmonics Rejection on Third-Generation Synchrotron Sources Using Compound Refractive Lenses*, *Journal of Synchrotron Radiation* **21**, 484 (2014).
- [22] S. P. Antipov *et al.*, *Rf Breakdown Test of Diamond-Loaded Resonator for High Gradient Wakefield Accelerator Applications*, *Diamond and Related Materials* **54**, 15 (2015).
- [23] S. V. Baryshev *et al.*, *White Light Interferometry for Quantitative Surface Characterization in Ion Sputtering Experiments*, *Applied Surface Science* **258**, 6963 (2012).